Use of contrast-enhanced ultrasonography to characterize adrenal gland tumors in dogs

Pascaline Pey, DVM, PhD; Federica Rossi, DVM; Massimo Vignoli, DVM, PhD; Luc Duchateau, PhD; Laurent Marescaux, DVM, PhD; Jimmy H. Saunders, DVM, PhD

Objective—To describe the contrast-enhanced ultrasonographic characteristics and vascular patterns of adrenal gland tumors in dogs and determine whether those features are indicative of malignancy or histologic type of tumor.

Animals—14 dogs with 16 adrenal gland lesions (10 carcinomas [8 dogs], 3 adenomas [3 dogs], and 3 pheochromocytomas [3 dogs]).

Procedures—Unsedated dogs with adrenal gland lesions underwent B-mode ultrasonography and contrast-enhanced ultrasonography ≤ 48 hours before adrenalectomy; contrast-enhanced ultrasonographic examinations were video-recorded. Macroscopic evaluation of the adrenal gland lesions and histologic examination of removed adrenal gland tissues were subsequently performed. Surgical and histopathologic findings and the ultrasonographic and contrast-enhanced ultrasonographic characteristics were recorded for the various tumor types. Time-intensity curves were generated from the contrast-enhanced ultrasonographic recordings and used to calculate regional blood volume (value proportional to area under the curve) and mean transit time (time the lesion began to enhance to the half-peak intensity).

Results—In adrenal gland carcinomas, tortuous feeding vessels were noticeable during the arterial and venous phases of contrast enhancement. Heterogeneity of contrast enhancement was evident only in malignant tumors. Compared with adenomas, adrenal gland carcinomas and pheochromocytomas had significantly less regional blood volume. Mean transit times were significantly shorter in adrenal gland carcinomas and pheochromocytomas than in adenomas.

Conclusions and Clinical Relevance—For dogs, evaluation of the vascular pattern and contrast-enhancement characteristics of adrenal gland tumors by means of contrast-enhanced ultrasonography may be useful in assessment of malignancy and tumor type. (*Am J Vet Res* 2014;75:886–892)

The most common adrenal gland neoplasms in dogs are adenomas, carcinomas, and pheochromocytomas.[1,2] Surgical treatment and perioperative complications depend on the type of tumor.[3–7] Results of imaging procedures are crucial for diagnosis and therapeutic planning. Diagnostic imaging of adrenal gland tumors provides important information regarding tumor localization and dimensions, contact with or invasion of neighboring organs or muscular tissue, vascular invasion, and potential for malignancy with possible prediction of histologic type.

Currently, ultrasonography and CT are most commonly used to investigate adrenal gland tumors. However, there are few criteria that allow a radiologist to estimate the potential malignancy and the histologic type of a tumor from those findings. Ultrasonography does not differentiate among types of adrenal gland tumors, but it has high specificity for detection of caudal vena cava invasion.[4,8–13] Computed tomography offers evaluation of the adrenal gland[14,15] and adrenal masses[16–19] in 3 planes. In dogs, contrast-enhanced CT enables accurate preoperative assessment of adrenal gland masses with a sensitivity and

Abbreviations

CEUS	Contrast-enhanced ultrasonography
MTT	Mean transit time
RBV	Regional blood volume
ROI	Region of interest

Received March 2, 2014.
Accepted June 9, 2014.
From the Departments of Medical Imaging of Domestic Animals and Orthopedy of Small Animals (Pey, Saunders) and Physiology and Biometry (Duchateau), Ghent University, 9820 Merelbeke, Belgium; Clinica Veterinaria dell'Orologio, via Gramsci, 1/4, 40037 Sasso Marconi (BO), Italy (Rossi, Vignoli); and Clinique vétérinaire oncovet, Avenue Paul Langevin, 59650 Villeneuve d'Ascq, France (Marescaux). Dr. Pey's present address is Department of Medical Imaging, Alfort Veterinary School, 94700 Maisons-alfort, France. Dr. Vignoli's present address is Clinica Veterinaria Modena Sud, Piazza dei Tintori 1, 41057 Spilamberto (MO), Italy.
This manuscript represents a portion of a thesis submitted by Dr. Pey to the University of Ghent Graduate School as partial fulfillment of the requirements for a Doctor in Veterinary Science degree.
No funding or conflict of interest to declare.
Presented in abstract form at the International Veterinary Radiology Association-European Association of Veterinary Diagnostic Imaging (IVRA-EAVDI) meeting, Bursa, Turkey, August 2012.
Address correspondence to Dr. Pey (pascaline_pey@hotmail.fr).

specificity for detection of vascular invasion (compared with surgery or necropsy) of 92% and 100%, respectively.[19] In ultrasonographic images, an adrenal gland that is > 4 cm in maximal thickness or width and that has irregular ill-defined contours and associated vascular invasion is a sign of malignancy.[8–12] When the contralateral adrenal gland is < 5 mm in maximal thickness or width, an adrenal gland mass is more likely to be a functioning epithelial tumor.[20] In dogs, the presence of calcification in the adrenal parenchyma is rarely encountered in pheochromocytomas but is often seen in adenomas or carcinomas and alone does not represent a sign of malignancy.[8–12] In humans, CEUS can be used to differentiate between adenomas and nonadenomatous lesions in adrenal glands.[21] The purpose of the study reported here was to describe the CEUS characteristics and vascular patterns of adrenal gland tumors in dogs and determine whether those features are indicative of malignancy or a histopathologic type of tumor.

Materials and Methods

Animals—Dogs with unilateral or bilateral adrenal gland lesions (detected by means of ultrasonography) were prospectively enrolled in the observational cross-sectional study, which was performed in accordance with the policies of the Animal Care Ethical Committee of Ghent University (EC2011/050). This was a multicenter study performed during 2011 and 2012. Dogs were included if they had a definitive histopathologic diagnosis of an adrenal gland tumor (determined on the basis of histologic examination of biopsy specimens). Within 48 hours prior to adrenalectomy, all dogs underwent physical examination followed by ultrasonography and then CEUS of the abnormal adrenal gland or glands. Sedation of the dogs was not required for ultrasonography and CEUS examinations. Following surgery, macroscopic analysis of the entire lesion was performed and then samples of the removed adrenal gland tissues underwent histologic examination. Dogs for which the final histopathologic diagnosis was equivocal were excluded from the study. The combination of surgical and histopathologic findings was considered as the gold standard for lesion description.

Preoperative B-mode ultrasonography—Each unsedated dog was placed in dorsal recumbency and examined by use of a 5-MHz linear or 5- to 8-MHz curved array transducer.[a] Ultrasonographic images were obtained in transverse and sagittal planes for both adrenal glands and recorded in Digital Imaging and Communications in Medicine (DICOM) format for further evaluation. A 20-gauge catheter was placed in a cephalic vein.

Preoperative CEUS—Immediately after the ultrasonographic examination, each unsedated dog was placed in dorsal recumbency and underwent a CEUS examination. This examination was performed by use of a 5-MHz linear transducer and a coded contrast-enhanced ultrasound method[b] with contrast-specific software. The mechanical index was 0.10, and the overall gain and time-gain compensation were adjusted as needed (range, 56% to 63%).

The contrast agent[c] was injected IV via the catheter in the cephalic vein. Each dog received a bolus of contrast agent (0.04 mL/kg) followed by injection of saline (0.9% NaCl) solution (3 mL). A timer was activated when injection of the contrast agent began.

For dogs with 1 adrenal gland lesion, a 2-injection procedure was used; for dogs with lesions in both adrenal glands, a 3-injection procedure was used. The first bolus of contrast agent was injected (at 0 minutes), and the adrenal gland lesion (or 1 of the 2 lesions) was examined ultrasonographically for 2 minutes. This examination was video-recorded but not used for further analysis. The ultrasonographic system was reset to the maximal acoustic pressure, and the cranial aspect of the abdomen was examined to remove any residual or trapped microbubbles before the next injection. Absence of a detectable signal from microbubbles within the abdominal aorta guaranteed the destruction of almost all circulating microbubbles that would create background noise during the examination after the second injection of contrast agent. The second injection was given 5 minutes after the first, and the adrenal gland lesion was again examined ultrasonographically for a period of 2 minutes. The video recording of the examination performed after the second injection was used for analysis.[22] For the dogs with 2 adrenal gland lesions, 1 of the 2 lesions was examined after the first and second injections. A third injection was given 5 minutes after the second injection, and the other adrenal gland lesion was examined ultrasonographically for a period of 2 minutes. This examination was video-recorded and used for further analysis.

For each CEUS examination, the arterial phase was defined as the interval from the detection of the contrast agent within the arteries visible on the image (ie, aorta and renal artery) to detection of contrast agent within the venous system (ie, caudal vena cava and phrenicoabdominal vein). The interval from visualization of the contrast agent within the venous system to the end of the examination was defined as the venous phase.

Surgery and histologic examination—Within 48 hours following completion of the preoperative examinations, each dog was anesthetized and underwent unilateral or bilateral adrenalectomy. First, macroscopic evaluation of the entire tumor was performed by a pathologist. Then, samples of the removed adrenal glands were routinely processed for histologic examination. The same pathologist evaluated each tumor and used established criteria to distinguish adrenocortical adenomas from carcinomas.[23]

Image analysis—Subjective and objective assessments of the recorded images were performed. B-mode ultrasonographic and CEUS images of each adrenal lesion were evaluated independently by 1 investigator (PP) and 1 of the clinical radiologists (JS, FR, MV, or LM) from the institution where the diagnosis had been made and treatment given. For the image evaluations, the observers used several criteria based on veterinary and human medical literature (**Appendix**). For each of the 16 lesions in the 14 dogs, height (dorsoventral dimension), width (mediolateral dimension), and length

Table 1—Mean ± SD height (dorsoventral dimension), width (mediolateral dimension), and length (craniocaudal dimension) determined from B-mode ultrasonographic images of 16 adrenal gland lesions in 14 dogs and height of the contralateral unaffected adrenal gland in 12 of those dogs.

	Lesion dimension (cm)			
	Affected adrenal gland			
Type of tumor	Height	Width	Length	Height of contralateral unaffected adrenal gland
Carcinoma	3.3 ± 2.3	3.6 ± 2.8	4.4 ± 2.1	1.1 ± 0.8
Adenoma	2.8 ± 1.5	2.4 ± 1.5	2.4 ± 1.2	0.7 ± 0.2
Pheochromocytoma	1.9 ± 0.6	1.9 ± 0.6	3.5 ± 0.8	0.6 ± 0.2

Among the 16 tumors, there were 10 carcinomas (n = 8 dogs), 3 adenomas (3), and 3 pheochromocytomas (3).

(craniocaudal dimension) were measured from the B-mode images. The relationship with adjacent structures was established. The appearance of the mass on pre- and postcontrast images was characterized from both B-mode and CEUS images. For the 12 dogs with unilateral adrenal gland lesions, the size and shape of the contralateral adrenal gland were also recorded for analysis. A consensus was reached between the investigator and the clinical radiologist in instances when any assessment differed.

A quantitative computerized analysis of the video-recorded CEUS images was then performed with dedicated software.[d] For dogs with unilateral adrenal gland tumors, the recording after the second contrast agent injection was analyzed; for dogs with bilateral adrenal gland tumors, the recording obtained from 1 lesion after the second contrast agent injection and the recording obtained from the other lesion after the third injection were analyzed. A closed polygon ROI was manually placed to encompass the entire tumor on the area included on the field of view. Image frames where the incorporated motion correction program was inefficient were deleted from the analysis. Time-intensity curves were generated, and perfusion variables (peak signal intensity, time to peak intensity, MTT, RBV, and regional blood flow) were calculated. Perfusion variables were defined as follows: peak signal intensity was the maximum intensity detected during the transit of the contrast agent bolus, time to peak intensity was the interval between the arrival of contrast agent in the adrenal vascularization and attainment of its maximum signal intensity, MTT was the time the lesion began to enhance to the half-peak intensity, RBV was a value proportional to the area under the time-intensity curve, and regional blood flow was the ratio of RBV to MTT.

Statistical analysis—Dimension data obtained from the B-mode ultrasonographic images of the 16 adrenal gland lesions in 14 dogs and height of the contralateral unaffected adrenal gland in 12 of those dogs were summarized as mean ± SD. The perfusion variables for the 3 tumor types were compared pairwise by use of the Wilcoxon rank sum test, and the data were summarized as median and the range. A value of $P < 0.05$ was considered significant. Statistical analysis was performed with software.[e]

Results

Dogs and adrenal gland lesions—Seventeen dogs were recruited initially; however, 3 were excluded because of an equivocal final histopathologic diagnosis. Fourteen dogs met the inclusion criteria. There were 6 large-breed, 5 medium-breed, and 3 small-breed dogs. Their median age was 10.5 years (range, 8 to 13 years). Among the 14 dogs, there were 9 males and 5 females. Twelve dogs were unilaterally affected, and 2 dogs were bilaterally affected; thus, 16 adrenal gland lesions were assessed. Among the lesions, there were 10 carcinomas (n = 8 dogs), 3 adenomas (3), and 3 pheochromocytomas (3); 10 left and 6 right adrenal glands were affected. Dimensions of the 16 adrenal gland lesions and 12 contralateral unaffected adrenal glands (in unilaterally affected dogs) varied widely (**Table 1**).

Carcinomas—On the basis of surgical and histopathologic findings, the adrenal gland carcinomas were characterized by the presence of 1 or several nodules or masses of variable size within the cortex and invading the capsule, multifocal hemorrhagic and necrotic areas, and extensive multifocal mineralization in some instances. Large tortuous vessels were observed. Tissues adjacent to an affected adrenal gland (ie, the ipsilateral kidney, pancreas, and adjacent muscles) were invaded in 3 dogs, and the caudal vena cava or the ipsilateral phrenicoabdominal vein was invaded in 4 dogs. This was seen during surgery and confirmed during histologic examination.

In B-mode ultrasonographic images, the parenchyma of all 10 carcinomas was hypoechoic, compared with the surrounding fat (**Figure 1**). Commonly, the parenchyma was heterogeneous (9/10 carcinomas); 4 of the 10 carcinomas had bright elements that cast strong acoustic shadows, which were interpreted as mineralization. In CEUS images, all 10 carcinomas had a poorly to moderately heterogeneous centripetal pattern of enhancement during the arterial and venous phases. Two enhancing patterns were observed; of the 10 carcinomas, 6 had poor contrast uptake with a bright peripheral halo and evidence of centripetal flow from the outer part of the halo to its inner part, and 4 had moderate contrast uptake with centripetal tortuous feeding vessels that were persistently visible during the arterial and venous phases. Histologic examination revealed

similar vessels in tissues sections of adrenal glands with carcinomas, and those vessels were presumed to be those detected with CEUS. Although vascular invasion was observed in the caudal vena cava or the ipsilateral phrenicoabdominal vein in 4 dogs during surgery and confirmed by histologic examination, neither imaging technique properly identified that vascular invasion in 3 dogs. However, tissues adjacent to the affected adrenal gland were invaded in 3 adrenal lesions, and in each instance, these invasions were suspected in ultrasonographic images and confirmed in CEUS images.

Adenomas—In the 3 dogs with a unilateral adrenal gland adenoma, the adrenal cortex was expanded by an encapsulated nodular neoplasm; dilated blood capillaries and multifocal areas of extramedullary hematopoiesis were observed on macroscopic evaluation of the adrenal lesions and histologic examination of excised tissues. Extensive multifocal mineralization was present in 1 adenoma. No vascular invasion was evident on the basis of surgical or histopathologic findings.

In B-mode ultrasonographic images, the parenchyma of the adenomas was either heterogeneously hypoechoic (2/3 adenomas) or homogeneously isoechoic (1/3 adenomas), compared with the surrounding fat (**Figure 2**). One adenoma was mineralized. In CEUS images, strong homogeneous centripetal contrast enhancement was observed in all 3 adenomas during the

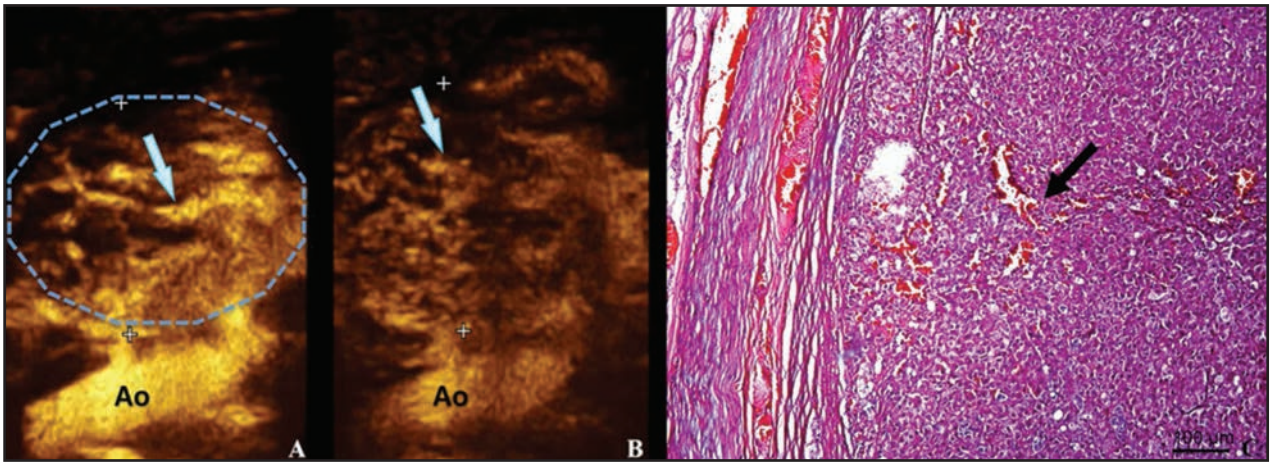

Figure 1—Selected images of a carcinoma of the left adrenal gland in a 6-year-old sexually intact male Yorkshire Terrier that had signs of hyperadrenocorticism. Contrast-enhanced ultrasonographic images (A and B) were obtained after IV injection of a bolus of contrast agent; the photomicrograph (C) was obtained after the adrenal gland had been subsequently removed and processed for histologic examination. The CEUS images in panels A and B represent the arterial phase (the interval between visualization of contrast agent within the imaged arteries and visualization of contrast agent within the venous system) and the venous phase (interval from visualization of the contrast agent within the venous system to the end of the examination [2 minutes after contrast agent injection]) of contrast enhancement. The blue dashed lines in panel A outline a representative ROI that was used for quantitative analysis. Immediately after contrast injection, contrast agent was detected in the aorta (Ao) and several tortuous feeding vessels (blue arrows in panels A and B) were identified in the center of the adrenal lesion (delimited by white crosses). Multiple areas were hypoechoic and unenhanced during the arterial phase (A); these areas remained unenhanced during the venous phase (B). In the section of affected adrenal gland tissue (C) from the approximate same location as the vessels in panels A and B, tortuous vessels (black arrow) and areas of hemorrhages are evident. H&E stain; bar = 100 µm.

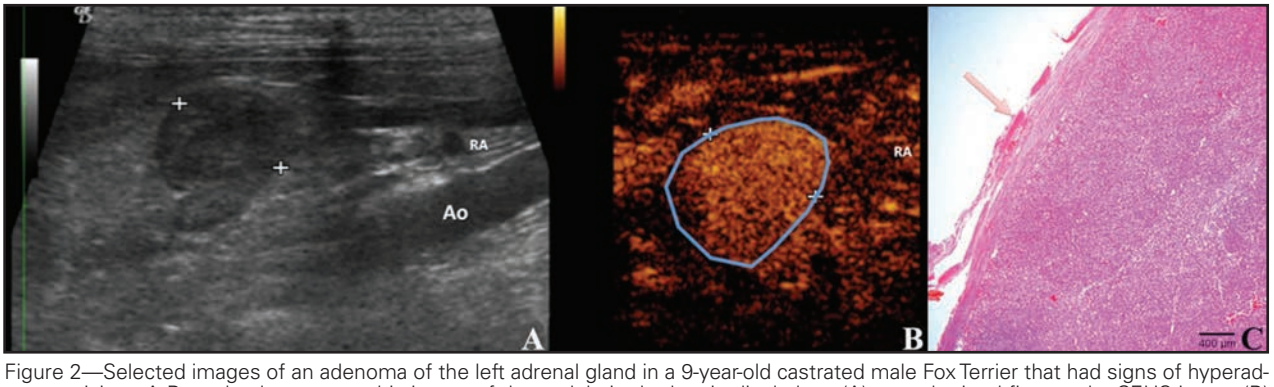

Figure 2—Selected images of an adenoma of the left adrenal gland in a 9-year-old castrated male Fox Terrier that had signs of hyperadrenocorticism. A B-mode ultrasonographic image of the nodule in the longitudinal plane (A) was obtained first, and a CEUS image (B) was then obtained after IV injection of a bolus of contrast agent; the photomicrograph (C) was obtained after the adrenal gland had been subsequently removed and processed for histologic examination. In the B-mode ultrasonographic image (A), the caudal pole of the left adrenal gland (delimited by white crosses) is deformed by the nodule; the nodule is rather homogeneous, it is smoothly outlined, and the hilus is still visible. The adrenal lesion is localized ventrally to the aorta (Ao) and cranially to the renal artery (RA). In the CEUS image (B), an intense homogeneous pattern of contrast enhancement is evident with no areas remaining hypoechoic. The blue continuous line in panel B outlines a representative ROI that was used for quantitative analysis. In the section of affected adrenal gland tissue that included the periphery of the adrenocortical adenoma (C), a hypervascularized capsule that surrounds a homogeneous cortical layer (orange arrow) is present. H&E stain; bar = 400 µm.

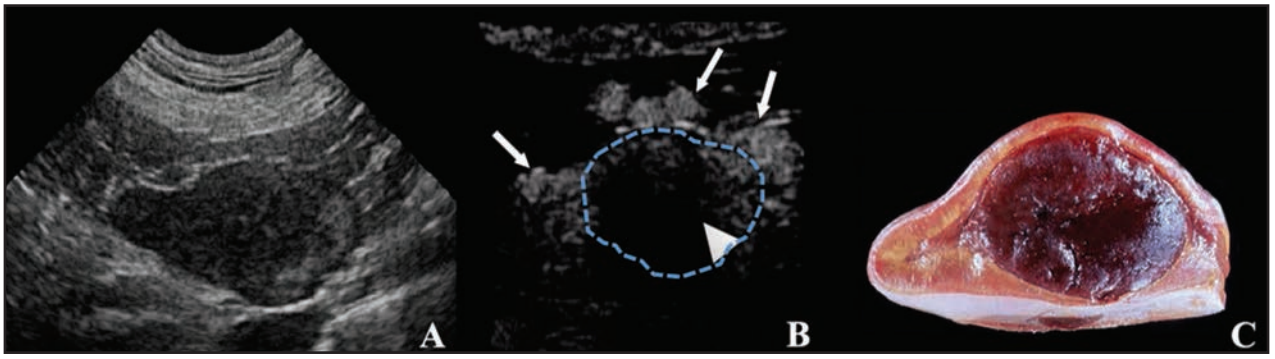

Figure 3—Selected images of a pheochromocytoma of the right adrenal gland detected incidentally in an 8-year-old sexually intact female Doberman Pinscher. A B-mode ultrasonographic image of the nodule in the longitudinal plane (A) was obtained first, and a CEUS image (B) was then obtained after IV injection of a bolus of contrast agent; the photograph (C) was obtained after the adrenal gland had been subsequently removed. In the B-mode ultrasonographic image (A), the caudal pole of the right adrenal gland is deformed by a large heterogeneous nodule with undulating borders. In the CEUS image (B), contrast uptake was detected in the tissues and vessels (arrows) surrounding the adrenal gland; no contrast enhancement was observed in the nodule (arrowhead). On the longitudinal cut surface of the excised adrenal gland (C), an extensive necrotic area is visible in the center of the mass that deforms the medulla of the caudal pole.

Table 2—Median (range) perfusion variables calculated from time-intensity curves generated from CEUS imaging data obtained for 16 adrenal gland lesions in the 14 dogs in Table 1.

	Type of tumor		
Variable	**Carcinoma**	**Adenoma**	**Pheochromocytoma**
Peak signal intensity (%)	24 (6–31)	30 (28–31)	15 (2–19)
Time to peak signal intensity (s)	18.5 (1.0–70.0)	21.0 (2.0–104.0)	5.0 (0.0–66.0)
RBV (grayscale level/s)	898.5[a] (114.0– 2,653.0)	2,845.0[b] (2,691.0–2,942.0)	140.0[a] (8.0–931.0)
Regional blood flow (grayscale level)	25 (7–42)	33 (24–43)	12 (3–22)
MTT (s)	28[a] (11–89)	87[b] (62–120)	6[a] (3–76)

Among the 16 tumors, there were 10 carcinomas (n = 8 dogs), 3 adenomas (3), and 3 pheochromocytomas (3).
[a,b] For RBV and MTT, values with different superscript letters differ significantly ($P < 0.05$).

arterial phase, and moderate enhancement was observed during the venous phase. No suspicion of vascular invasion was evident with either of the imaging techniques.

Pheochromocytomas—In the 3 dogs with a unilateral pheochromocytoma, a multilobular lesion that was located in the adrenal medulla and compressed the cortex was detected during surgery and confirmed by histologic examination of excised tissues. There were multifocal hemorrhagic and necrotic areas with invasion of the phrenicoabdominal vein in 2 dogs and no invasion of adjacent tissues in any of the 3 dogs.

In B-mode ultrasonographic images, the parenchyma of all 3 pheochromocytomas was hypoechoic, compared with the surrounding fat (**Figure 3**). The parenchyma was homogeneous (1/3 pheochromocytomas) or heterogeneous (2/3 pheochromocytomas) with no mineralization. In CEUS images, 2 pheochromocytomas had almost no contrast enhancement centrally and moderate enhancement in periphery during the arterial and venous phases; the other had strong centrifugal contrast enhancement during the arterial phase and poor enhancement during the venous phase. Vascular invasion was observed in 2 of the 3 dogs during surgery, but that invasion was detected with CEUS in only 1 of those 2 dogs.

Perfusion variables—From the data obtained during CEUS, time-intensity curves were generated and perfusion variables were determined (**Table 2**). Only RBV and MTT differed among the types of adrenal gland tumor. The RBVs of carcinomas and pheochromocytomas were significantly lower than the RBV of adenomas ($P = 0.014$ and $P = 0.005$, respectively); there was no difference ($P = 0.368$) between the RBV of carcinomas and that of pheochromocytomas. Similarly, the MTTs of carcinomas and pheochromocytomas were significantly shorter than the MTT of adenomas ($P = 0.045$ and $P = 0.048$, respectively). Although not significantly different, the mean time to peak signal intensity of benign lesions (ie, adenomas [42.3 seconds]) was almost twice the time to peak signal intensity of malignant lesions (ie, carcinomas [24.2 seconds] or pheochromocytomas [23.7 seconds]).

Discussion

Contrast-enhanced ultrasonography of the 10 adrenal gland carcinomas examined in the present study revealed 2 contrast-enhancing patterns. One pattern was characterized by poor centripetal contrast agent uptake with a bright peripheral halo, which corresponded to histopathologic findings of a large central necrotic area surrounded by peripheral neoplastic tissue. In general, the hypoperfused areas correlated

grossly with areas of necrosis or hemorrhage. The other pattern was characterized by an intense heterogeneous contrast uptake within a persistently visible tortuous centripetal arterial vessel, likely resulting from tumor neoangiogenesis. Similar vessels were identified on histologic examination of removed tissues and were presumed to be those detected with CEUS on the basis of gross mapping. A similar feature has been described to be highly suggestive of malignancy in splenic lesions.[24] Contrast-enhanced ultrasonography aided in the real-time observation of tortuous feeding vessels.

In histopathologic reports,[2,25,26] areas of extramedullary hematopoiesis in adenomas are frequently described. This histologic feature could explain the hypoechoic (compared with the surrounding fat) and heterogeneous appearance of some adenomas in B-mode ultrasonographic images. In CEUS images, a strong homogeneous contrast enhancement was observed. Homogeneity of the enhancement was therefore consistent with a benign lesion. In the present study, 1 dog had a unilateral adrenal gland adenoma with mineralization, yet it was still possible to detect this homogeneity in enhancement in the parenchyma surrounding the acoustic shadow cast by the mineralization.

On histologic examination, a pheochromocytoma may have necrotic or hemorrhagic areas or cystic cavities.[2,12,25,26] In the present study, CEUS of 2 of the 3 pheochromocytomas revealed no central contrast enhancement, which was interpreted as necrosis or hemorrhage, and moderate peripheral enhancement. The central hypoperfused areas detected with CEUS corresponded histologically to areas of necrosis in those adrenal glands. The remaining pheochromocytoma that had homogeneous contrast enhancement did not meet histologic criteria for malignancy. It is known that some pheochromocytomas have a more benign biological behavior than other apparently malignant pheochromocytomas,[26] and homogeneous contrast enhancement may be more consistent with benign tumor behavior.

A centripetal pattern of contrast enhancement was observed in the adrenal gland adenomas and carcinomas in the dogs of the present study. We recently reported that, in dogs, an adrenal gland that is apparently healthy or an adrenal gland that is hyperplastic as a result of pituitary-dependent hyperadrenocorticism has a centrifugal pattern of contrast enhancement.[27,28] In a dog in which nodular enlargement of an adrenal gland pole or an equivocal asymmetry of its 2 adrenal glands is evident, results of CEUS may be useful in predicting whether these changes are attributable to nodular hyperplasia, adenoma, or carcinoma; if a centripetal contrast-enhancing pattern is detected, the diagnosis may more likely be adrenal gland adenoma or carcinoma. However, additional validating studies should be performed to determine whether the pattern of contrast enhancement could be used to differentiate adrenal gland nodular hyperplasia from adenoma or carcinoma, because a centrifugal pattern of contrast enhancement was detected in 1 of the 3 pheochromocytomas examined in the present study. In pheochromocytomas, the vascularization is more intense in the medulla and can accentuate the centrifugal pattern. In the absence of clinical or biological signs of adrenal gland disease, it may be difficult to differentiate the contrast enhancement patterns in small nodules, regardless of whether they are malignant or benign.

Among the types of adrenal gland tumor assessed in the dogs of the present study, the RBVs and the MTTs in carcinomas and pheochromocytomas were decreased, compared with findings for adenomas. Blood volume in malignant lesions may be smaller than that in benign lesions because of the presence of large necrotic areas that diminish the perfused volume. In addition, blood may also pass more quickly through the malignant tumors because of the presence of neovessels that are small in diameter and short in length and that generate faster blood velocity in a large part of the tumor.[2,12,26]

The present study had several limitations. The first limitation was the small number of dogs, but the recruitment of dogs with adrenal gland tumors was inherently challenging. The main weakness in the study protocol was the absence of a more validated technique of histologic mapping. Although only gross manual mapping of the lesions was performed, we assumed that the largest lesions or vessels detected on histologic examination corresponded to the lesions visible on the recorded images.

The results of the present study indicated that there are some ultrasonographic features of adrenal gland tumors in dogs that may be tumor-type specific. Given the persistent tortuous vessels observed in adrenal gland carcinomas or the heterogeneity of the contrast enhancement only observed in malignant tumors, CEUS images may be useful for predicting malignancy of adrenal gland lesions and determining the type of adrenal gland tumors in dogs.

a. CnTI Mylab 30 or 70, Esaote, Firenze, Italy.
b. CnTI Megas Esatune, Esaote, Firenze, Italy.
c. Sonovue, Bracco Imaging, Milano, Italy.
d. Qontrast, Bracco Imaging, Milano, Italy.
e. SAS, version 9.2, SAS Institute Inc, Cary, NC.

References

1. Feldman EC, Nelson RW. The adrenal gland. In: Feldman EC, Nelson RW, eds. *Canine and feline endocrinology and reproduction*. 3rd ed. Philadelphia: WB Saunders Co, 2004;251–484.
2. Capen CC. Endocrine glands. In: Maxie MG, ed. *Jubb, Kennedy and Palmer's pathology of domestic animals*. 5th ed. Philadelphia: Elsevier Saunders, 2007;325–428.
3. Anderson CR, Birchard SJ, Powers BE, et al. Surgical treatment of adrenocortical tumors: 21 cases (1990–1996). *J Am Anim Hosp Assoc* 2001;37:93–97.
4. Kyles AE, Feldman EC, De Cock HEV, et al. Surgical management of adrenal gland tumors with and without associated tumor thrombi in dogs: 40 cases (1994–2001). *J Am Vet Med Assoc* 2003;223:654–662.
5. Schwartz P, Kovak JR, Koprowski A, et al. Evaluation of prognostic factors in the surgical treatment of adrenal gland tumors in dogs: 41 cases (1999–2005). *J Am Vet Med Assoc* 2008;232:77–84.
6. De Brito Galvao JF, Chew DJ. Metabolic complications of endocrine surgery in companion animals. *Vet Clin North Am Small Anim Pract* 2011;41:847–868.
7. Massari F, Nicoli S, Romanelli G, et al. Adrenalectomy in dogs with adrenal gland tumors: 52 cases (2002–2008). *J Am Vet Med Assoc* 2011;239:216–221.

8. Reusch C, Feldman EC. Canine hyperadrenocorticism due to adrenocortical neoplasia: pretreatment evaluation of 41 dogs. *J Vet Intern Med* 1991;5:3–10.
9. Barthez PY, Marks SL, Woo J, et al. Pheochromocytoma in dogs: 61 cases (1984–1995). *J Vet Intern Med* 1997;11:272–278.
10. Besso JG, Penninck DG, Gliatto JM. Retrospective ultrasonographic evaluation of adrenal lesions in 26 dogs. *Vet Radiol Ultrasound* 1997;38:448–455.
11. Hoerauf A, Reusch CE. Ultrasonographic characteristics of both adrenal glands in 15 dogs with functional adrenocortical tumors. *J Am Anim Hosp Assoc* 1999;51:193–199.
12. Rosenstein DS. Diagnostic imaging in canine pheochromocytoma. *Vet Radiol Ultrasound* 2000;41:499–506.
13. Davis MK, Schochet RA, Wrigley R. Ultrasonographic identification of vascular invasion by adrenal tumors in dogs. *Vet Radiol Ultrasound* 2012;53:442–445.
14. Bertolini G, Furlanello T, De Lorenzi D, et al. Computed tomographic quantification of canine adrenal gland volume and attenuation. *Vet Radiol Ultrasound* 2006;47:444–448.
15. Bertolini G, Furlanello T, Drigo M, et al. Computed tomographic adrenal gland quantification in canine adrenocorticotroph hormone-dependent hyperadrenocorticism. *Vet Radiol Ultrasound* 2008;49:449–453.
16. Emms SG, Wortman JA, Johnston DE, et al. Evaluation of canine hyperadrenocorticism, using computed tomography. *J Am Vet Med Assoc* 1986;189:432–439.
17. Voorhout G, Stolp R, Lubberink AA, et al. Computed tomography in the diagnosis of canine hyperadrenocorticism not suppressible by dexamethasone. J *Am Vet Med Assoc* 1988;192:641–646.
18. Voorhout G, Stolp R, Rijnberk A, et al. Assessment of survey radiography and comparison with x-ray computed tomography for detection of hyperfunctioning adrenocortical tumors in dogs. *J Am Vet Med Assoc* 1990;196:1799–1803.
19. Schultz RM, Wisner ER, Johnson EG, et al. Contrast-enhanced computed tomography as a preoperative indicator of vascular invasion from adrenal masses in dogs. *Vet Radiol Ultrasound* 2009;50:625–629.
20. Benchekroun G, de Fornel-Thibaud P, Rodríguez Piñeiro MI, et al. Ultrasonography criteria for differentiating ACTH dependency from ACTH independency in 47 dogs with hyperadrenocorticism and equivocal adrenal asymmetry. *J Vet Intern Med* 2010;24:1077–1085.
21. Friedrich-Rust M, Schneider G, Bohle RM, et al. Contrast-enhanced sonography of adrenal masses: differentiation of adenomas and nonadenomatous lesions. *AJR Am J Roentgenol* 2008;191:1852–1860.
22. Tang MX, Mulvana H, Gauthier T, et al. Quantitative contrast-enhanced ultrasound imaging: a review of sources of variability. *Interface Focus* 2011;1:520–539.
23. Labelle P, Kyles AE, Farver TB, et al. Indicators of malignancy of canine adrenocortical tumors: histopathology and proliferation index. *Vet Pathol* 2004;41:490–497.
24. Taeymans O, Penninck D. Contrast enhanced ultrasonographic assessment of feeding vessels as a discriminator between malignant vs. benign focal splenic lesions. *Vet Radiol Ultrasound* 2011;52:457–461.
25. Kelly DF, Siegel ET, Berg P. The adrenal gland in dogs with hyperadrenocorticalism: a pathologic study. *Vet Pathol* 1971;8:385–400.
26. Capen CC. Tumors of the endocrine glands. In: Meuten DJ, ed. *Tumors in domestic animals*. 4th ed. Ames, Iowa: Blackwell Publishing Co, 2002;629–637.
27. Pey P, Vignoli M, Haers H, et al. Contrast-enhanced ultrasonography of the normal canine adrenal gland. *Vet Radiol Ultrasound* 2011;52:560–567.
28. Pey P, Daminet S, Smets PMY, et al. Contrast-enhanced ultrasonography of adrenal glands in dogs with pituitary dependent hypercortisolism. *Am J Vet Res* 2013;74:417–425.

Appendix

Criteria used to evaluate B-mode ultrasonographic and CEUS images of adrenal gland lesions in dogs.

Variable	Description
Adrenal gland affected	Left or right
Size of lesion	Height (dorsoventral; cm), width (mediolateral; cm), and length (craniocaudal; cm)
Size of contralateral adrenal gland	Height (cm)
Focal or diffuse distribution	Focal enlargement (nodule) or mass (effacement of the adrenal gland hilus)
Relationship of lesion with caudal vena cava	
Mass effect	Yes or no
Contact	Yes or no
Invasion	Yes or no
Relationship of lesion with adjacent organ or tissue	
Mass effect	Yes or no
Contact	Yes or no
Invasion	Yes or no
Invasion of phrenicoabdominal vein	Yes or no
Nonenhanced ultrasonographic appearance of lesion	Hypoechoic, isoechoic, or hyperechoic, compared with surrounding tissues*; acoustic shadowing (yes or no); and homogeneous or heterogeneous pattern
CEUS appearance of lesion	Poor or strong contrast enhancement, homogeneous or heterogeneous contrast enhancement, or centrifugal or centripetal enhancement pattern
Margin of lesion	Clear delineation or poor definition and smooth or irregular outline

*Echogenicity was compared with echogenicity of the surrounding fat.